Electronic Supplementary Material (ESI) for Energy & Environmental Science

Supporting Information For:

Photocatalytic Water Oxidation by Very Small Cobalt Domains on a Silica Surface

Hyun S. Ahn, Junko Yano, and T. Don Tilley*

Contribution from the Department of Chemistry University of California, Berkeley, Berkeley, California 94720, and the Chemical Sciences Division, Lawrence Berkeley National Laboratory, 1 Cyclotron Road, Berkeley, California, 94720.

Email: tdtilley@berkeley.edu

Quantification of surface Si-OH sites on SBA-15

Quantification of surface Si-OH sites on SBA-15 was conducted following a published method from this laboratory.[1] The reaction of $Mg(CH_2Ph)_2{\cdot}2THF$ with silica surface produces surface bound magnesium species and an equivalent of toluene, which then can be quantified by ^1H NMR spectroscopy. An average of 1.2 nm^{-2} Si-OH groups was measured in the SBA-15 samples used in this report.

Calculation of the theoretical maximum loading of cobalt on SBA-15

As described above, ca. 1.2 nm^{-2} Si-OH groups are surface accessible in the SBA-15 material used in this work. With the specific surface area of 634 $m^2{\cdot}g^{-1}$, the total number of Si-OH sites is ca. 7.61×10^{20}. Because each surface grafted cobalt species is bipodal and consumes two Si-OH sites, the maximum possible number of cobalt atoms that can be surface bound is 3.80×10^{20}. Multiplying this number by the atomic mass of cobalt and dividing by the Avogadro's number yields 0.0372, that is the theoretical maximum weight fraction of cobalt per gram of SBA-15 material. Expressed in a mathematical form:

$$1.2\ \frac{\mathrm{SiOH}}{\mathrm{nm}^2} \times \left[6.34 \times 10^{20}\ \frac{\mathrm{nm}^2}{\mathrm{g}}\right] \times \frac{\mathrm{Surface\ Co}}{2\ \mathrm{SiOH}} = [3.80 \times 10^{20}]\ \mathrm{Co/g}$$

$$[3.80 \times 10^{20}]\,\frac{\mathrm{Co}}{\mathrm{g}} \times 58.933\ \frac{\mathrm{g}}{\mathrm{mol\ Co}} \times \left[\frac{1}{6.022 \times 10^{23}}\right] \frac{\mathrm{mol\ Co}}{\mathrm{Co}}$$

$$= 0.0372\ \ \mathrm{mass\ fraction\ of\ Co\ per\ gram\ of\ material}$$

Turnover frequency (TOF) calculation

Turnover frequencies (TOF) for CoSBA catalysts were calculated by first converting the amount of oxygen formed into turnover numbers (TON) by dividing the amount of O_2 by the total number of cobalts in the catalysis reaction. This is the absolute lower limit for TOF, since all cobalt atoms in the reaction vessel are assumed to participate in the reaction. These TON values were then plotted against time, as shown in Figure S1, and the slope of the tangent line to the initial linear growth region of the plot (shown in blue lines in Figure S1) was taken to be the TOF of the catalyst. Typically 250 – 300 data points were selected in determining the slope. A sample calculation is as follows:

$$45\ \mu\text{mol O}_2 \times \left[0.040\ \text{g catalyst} \times 0.0048\ \text{wt\% Co} \times \frac{1 \times 10^6\ \mu\text{mol Co}}{58.933\ \text{g Co}}\right]^{-1}$$

$$= 13.8\ \text{Turnovers}$$

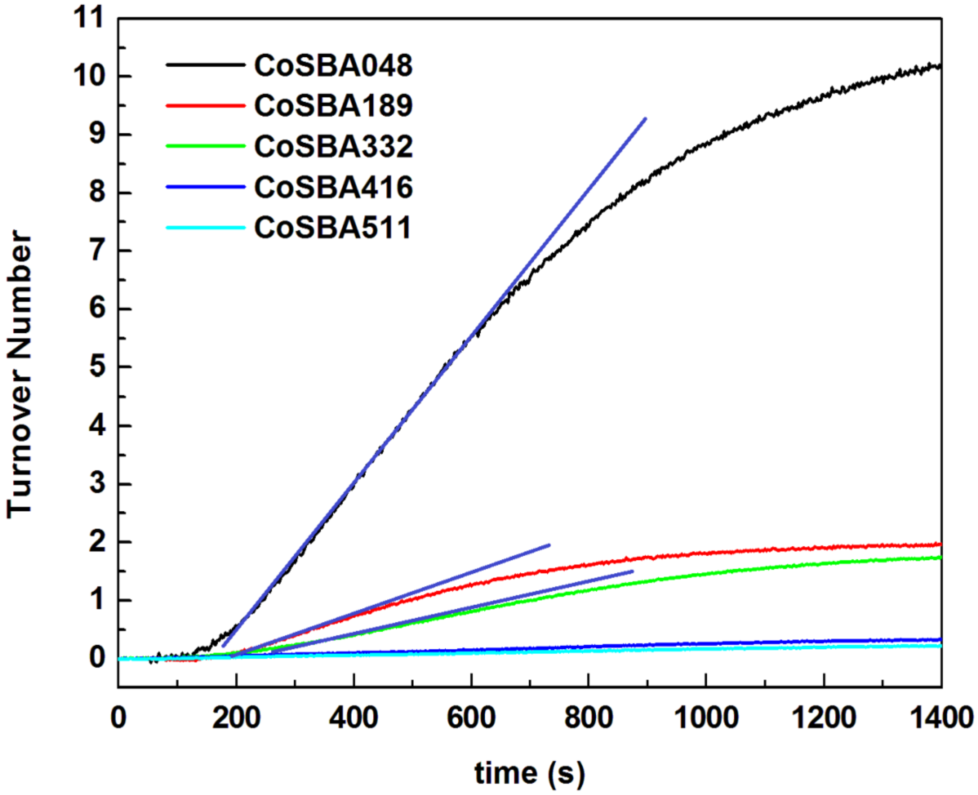

Figure S1. Catalytic turnover numbers as functions of time for selected CoSBA samples. Tangent lines to the initial onset of catalyses were depicted in blue, the slope of which represents the TOF$_i$ of the catalyst (TON·time^{-1}).

EXAFS Curve Fitting

X-ray absorption data treatment and EXAFS fitting were performed using Athena and Artemis programs in the Ifeffit software package. The goodness of the fits was evaluated by the EXAFS R-factors (R_f), which indicate the difference between data and theory. Evaluation of different fits to others was conducted by using the reduced χ_v^2 as described in literature.[2-4]

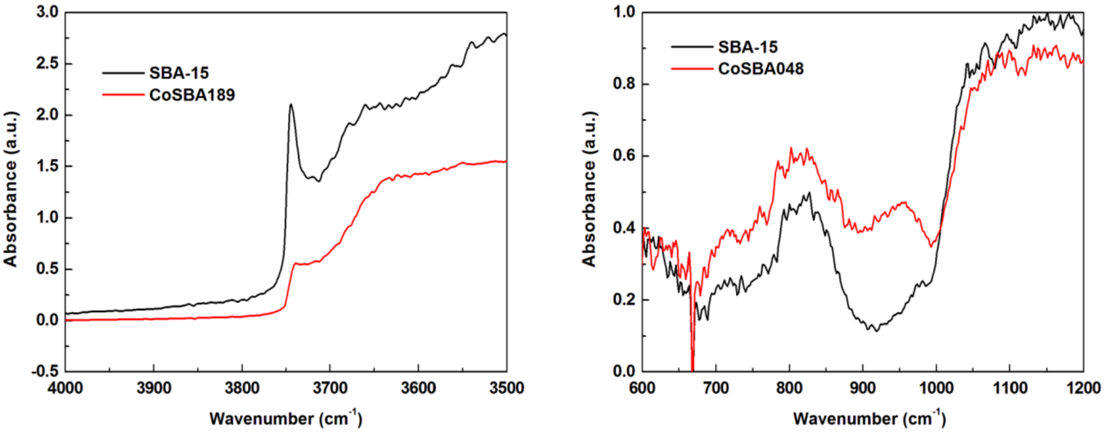

Figure S2. Selected regions in the diffuse reflectance FTIR spectra of CoSBA materials are displayed referenced to the parent SBA-15. Diminishing of SiO-H vibration at ca. 3750 cm^{-1} with concomitant appearance of Co-O-Si vibration at ca. 940 cm^{-1}suggests that the cobalt centers on CoSBA materials are covalently binding to the surface via the consumption of surface Si-OH groups.

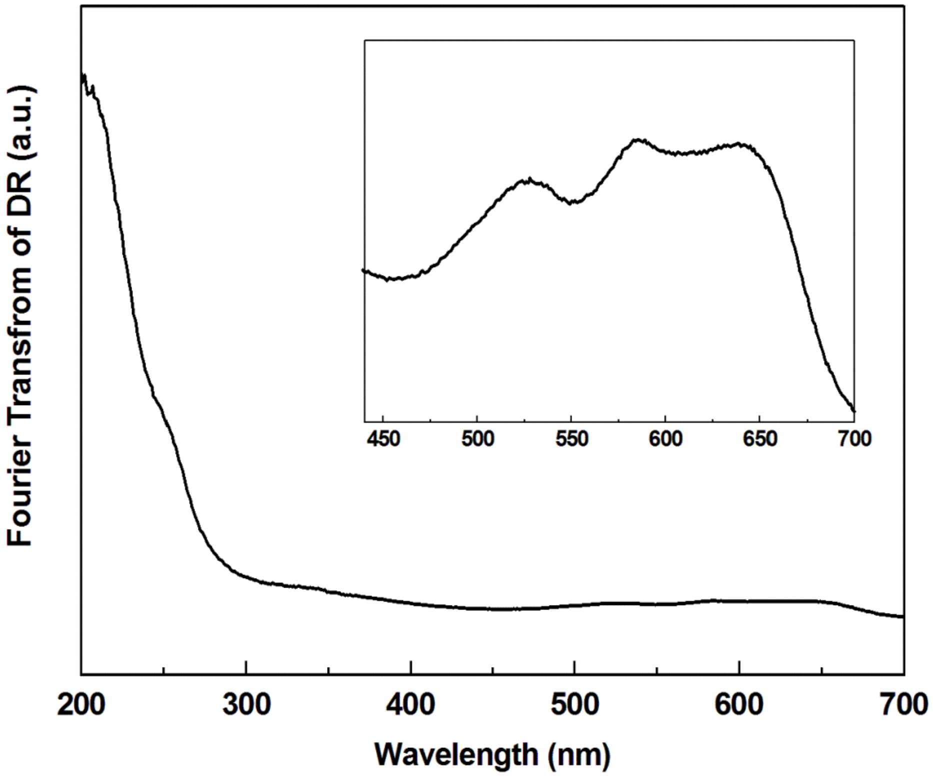

Figure S3. Diffuse reflectance UV-vis spectrum of CoSBA189 is displayed. The three peaks in the d-d transition region at 530, 580, and 650 nm are indicative of T_d Co^{II} centers.

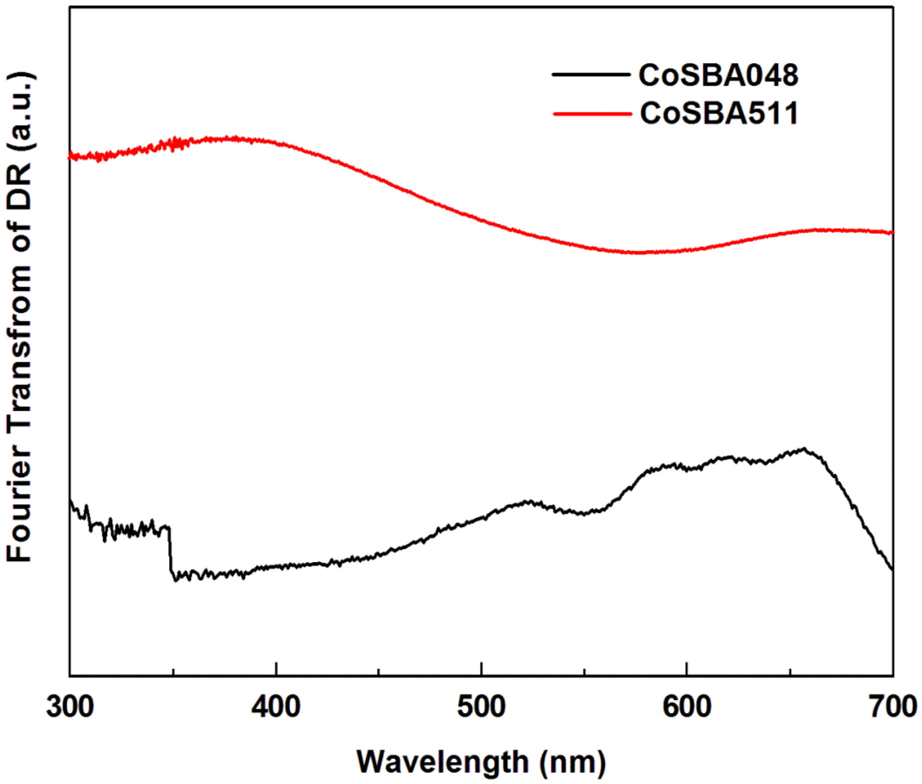

Figure S4. Diffuse reflectance UV-vis spectrum of CoSBA511 is displayed along with that of CoSBA048. The broad band centered around 350 nm is characteristic of Co_3O_4.

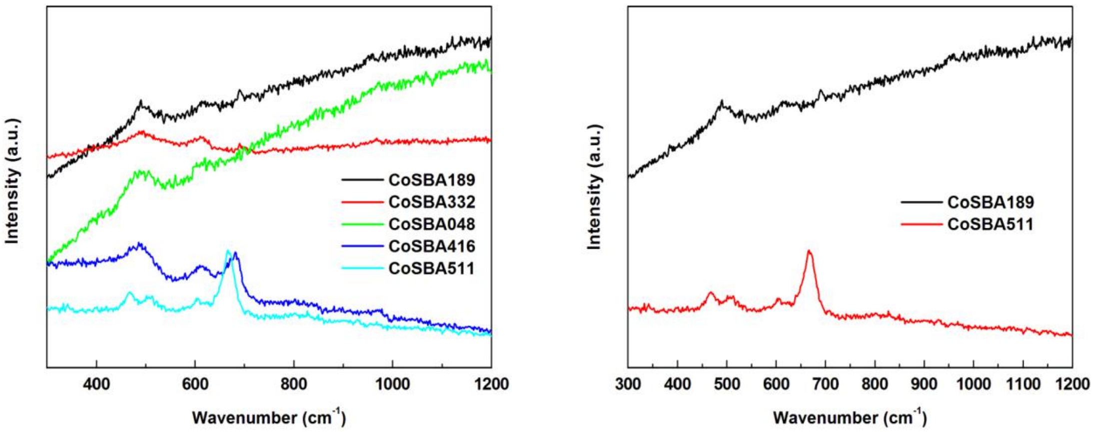

Figure S5. Raman spectra of CoSBA materials. Broad vibration centered at 500 cm^{-1} was observed for CoSBA samples of lower loading, where as peaks at 485, 505, and 691 cm^{-1} (indicative of Co_3O_4) were observed for CoSBA416 and CoSBA511.

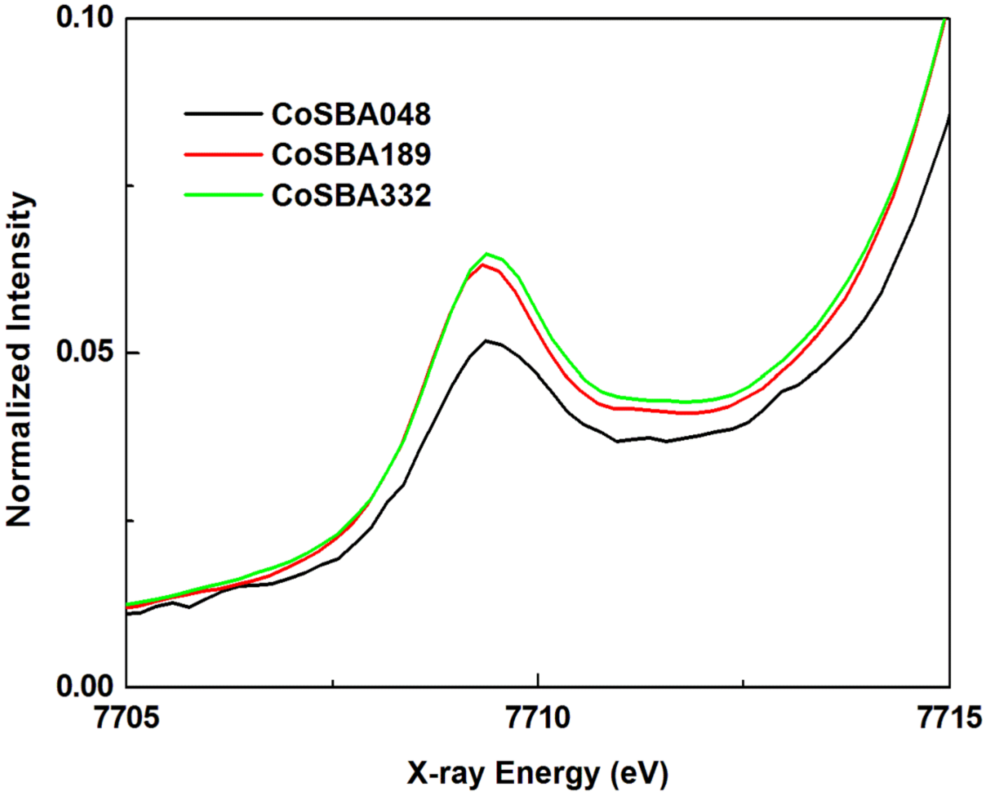

Figure S6. Pre-edge feature at 7709 eV was observed in the XANES spectra of low loading CoSBA samples, indicating the Co^{II} centers are in noncentrosymmetric (T_d) coordination environments. (CoSBA048, 189, and 332 shown, since these samples collected at the ALS showed more clearly the pre-edge peaks than those of CoSBA027 and CoSBA106 collected at SSRL).

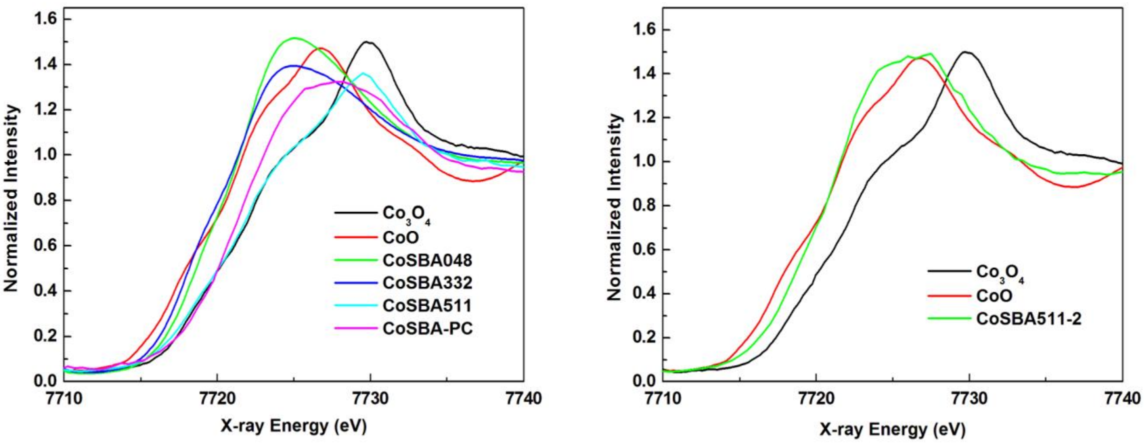

Figure S7. XANES spectra of CoSBA materials are displayed on the left. XANES of CoSBA511 closely resembles that of Co_3O_4, suggesting that small domains of Co_3O_4 were formed. On the right, however, XANES of a different part of CoSBA511 resembles those of lower loading CoSBA samples, exhibiting inhomogeneity in the material unlike any other CoSBA materials.

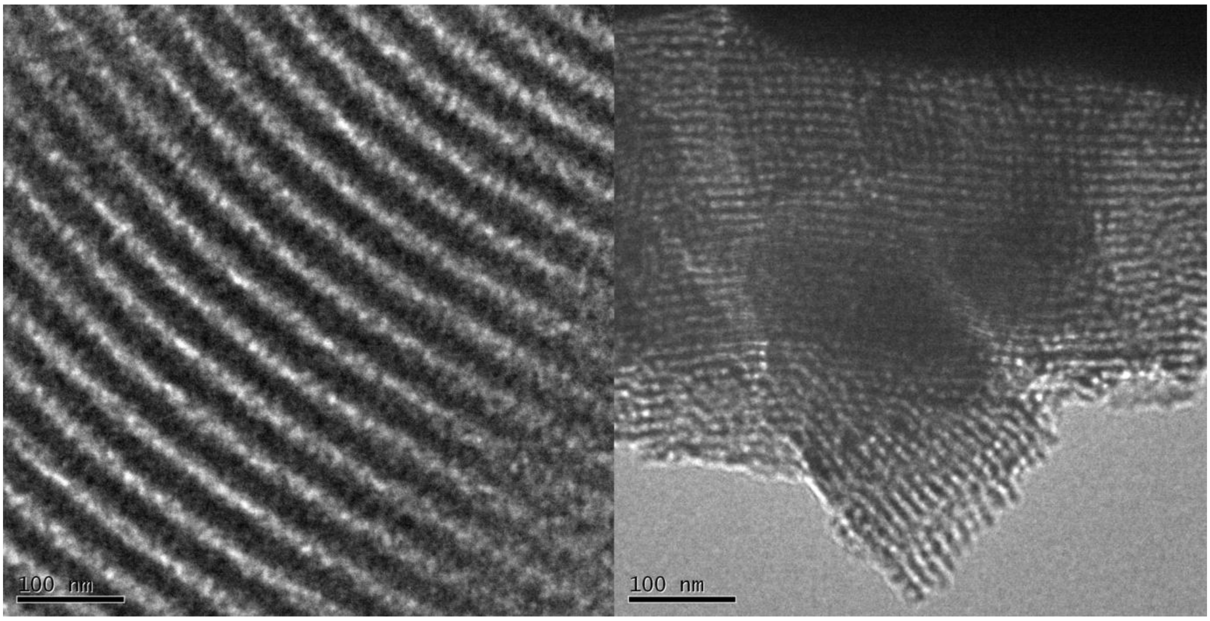

Figure S8. TEM images of CoSBA416 and CoSBA511 samples. Even at the highest of loadings no blockage of pores or visible particle formation was observed.

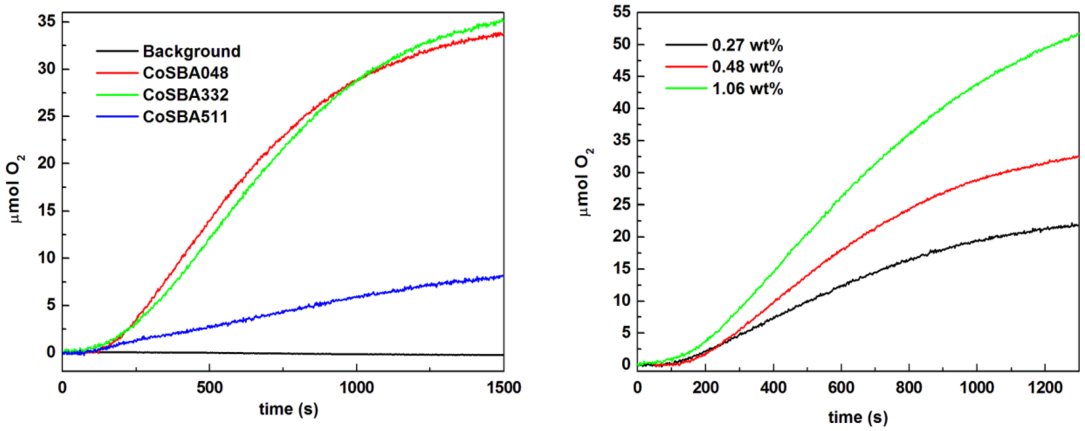

Figure S9. Oxygen evolution with time is plotted above. As seen on the right, overall product formation grows linearly with increasing surface concentration of cobalt. On the left, it is seen that the background (SBA-15) slowly drops below zero over time due to the evolution of CO_2 from bicarbonate buffer and the decomposition of $Ru(bpy)_3^{2+}$, assuring that the reaction vessel was gas-tight and the oxygen penetration from the atmosphere was negligible.

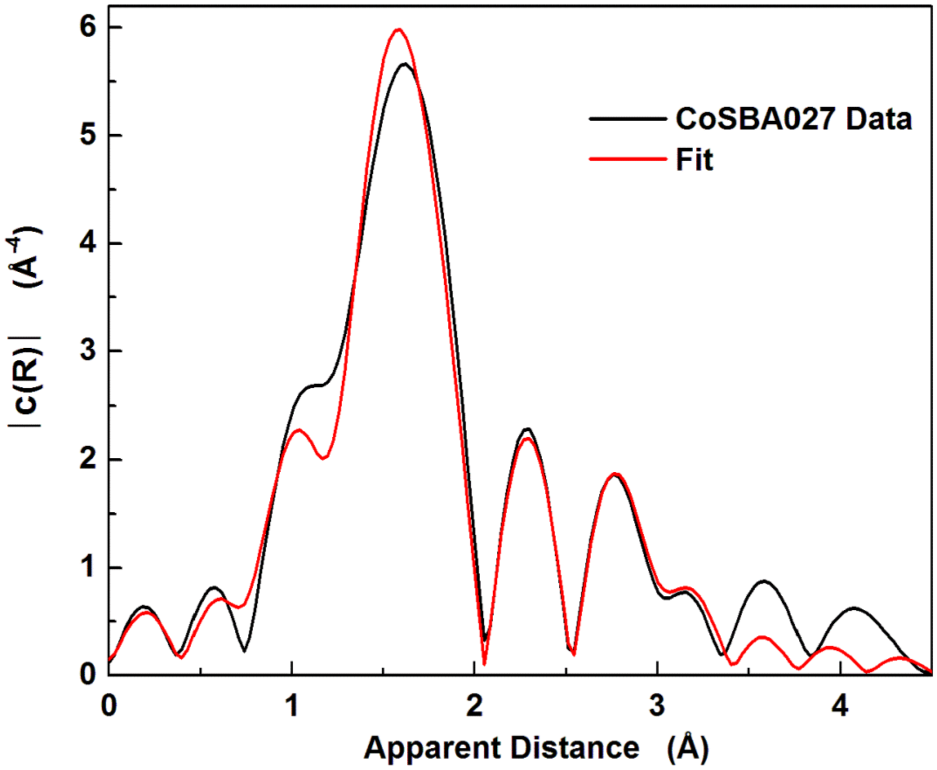

Figure S10. EXAFS fit of CoSBA027 is displayed (also shown in Figure 3). The EXAFS R-factor (R_f) for the fit is 0.0016 and the reduced χ_v^2 is 32.9. Co-O distance in this model is 2.07 Å with a coordination number (CN) of 5. Co-Si distance in this model is 3.26 Å with a CN of 2. Co-Co distance in this model is 2.82 Å with a CN of 0.4.

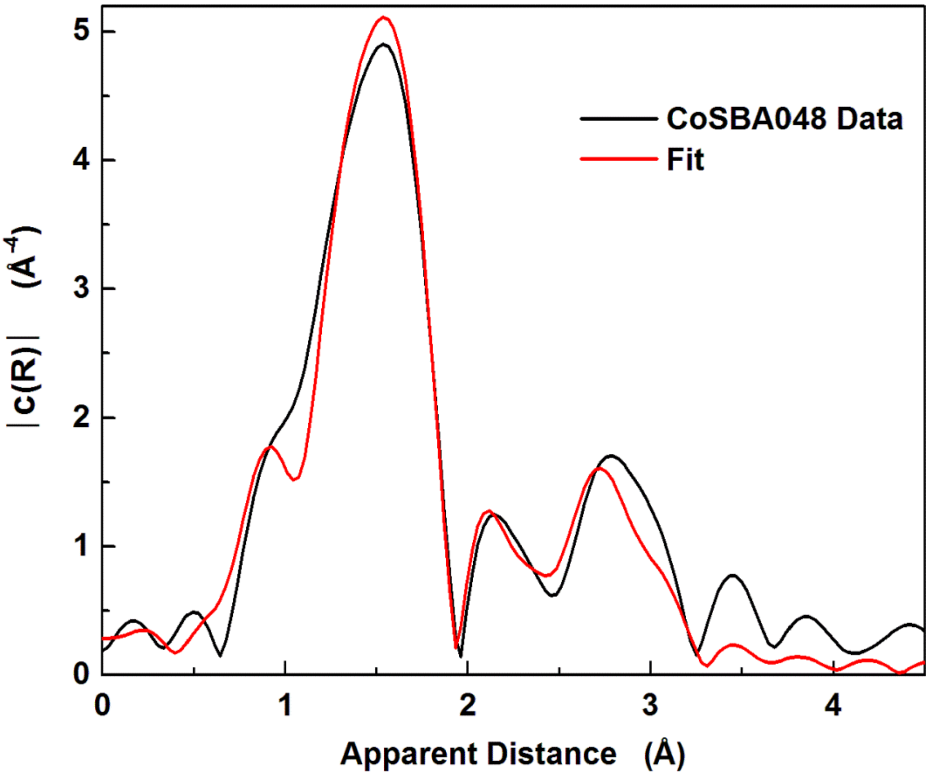

Figure S11. EXAFS fit of CoSBA048 is displayed. The EXAFS R-factor (R_f) for the fit is 0.0053 and the reduced χ_v^2 is 42.8. Co-O distance in this model is 2.04 Å with a coordination number (CN) of 5. Co-Si distance in this model is 3.27 Å with a CN of 2. Co-Co distance in this model is 2.93 Å with a CN of 0.5.

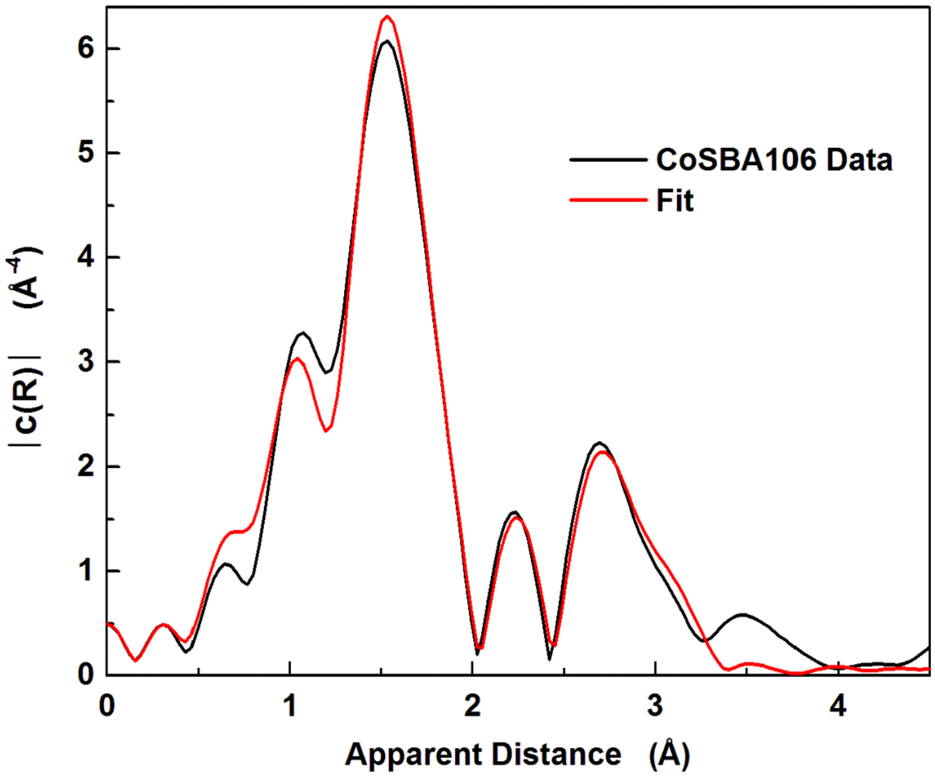

Figure S12. EXAFS fit of CoSBA106 is displayed. The EXAFS R-factor (R_f) for the fit is 0.0043 and the reduced χ_v^2 is 9.3. Co-O distance in this model is 2.09 Å with a coordination number (CN) of 5. Co-Si distance in this model is 3.29 Å with a CN of 2. Co-Co distance in this model is 2.89 Å with a CN of 1.2.

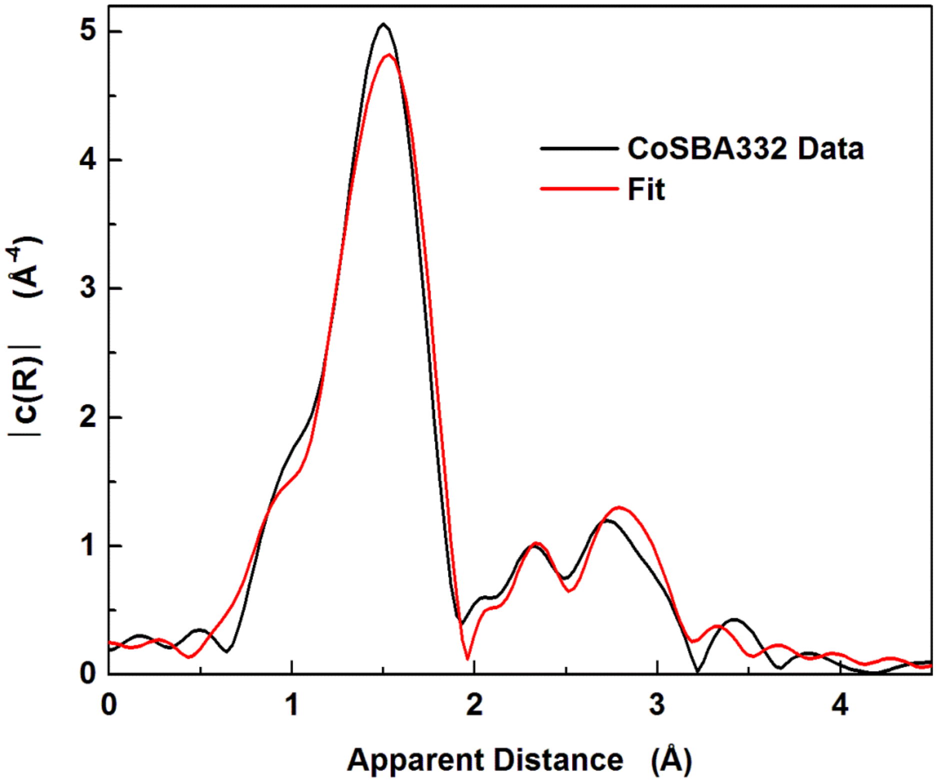

Figure S13. EXAFS fit of CoSBA332 is displayed. The EXAFS R-factor (R_f) for the fit is 0.0068 and the reduced χ_v^2 is 65.7. Co-O distance in this model is 2.02 Å with a coordination number (CN) of 5. Co-Si distance in this model is 3.12 Å with a CN of 2. Co-Co distance in this model is 3.04 Å with a CN of 2.3.

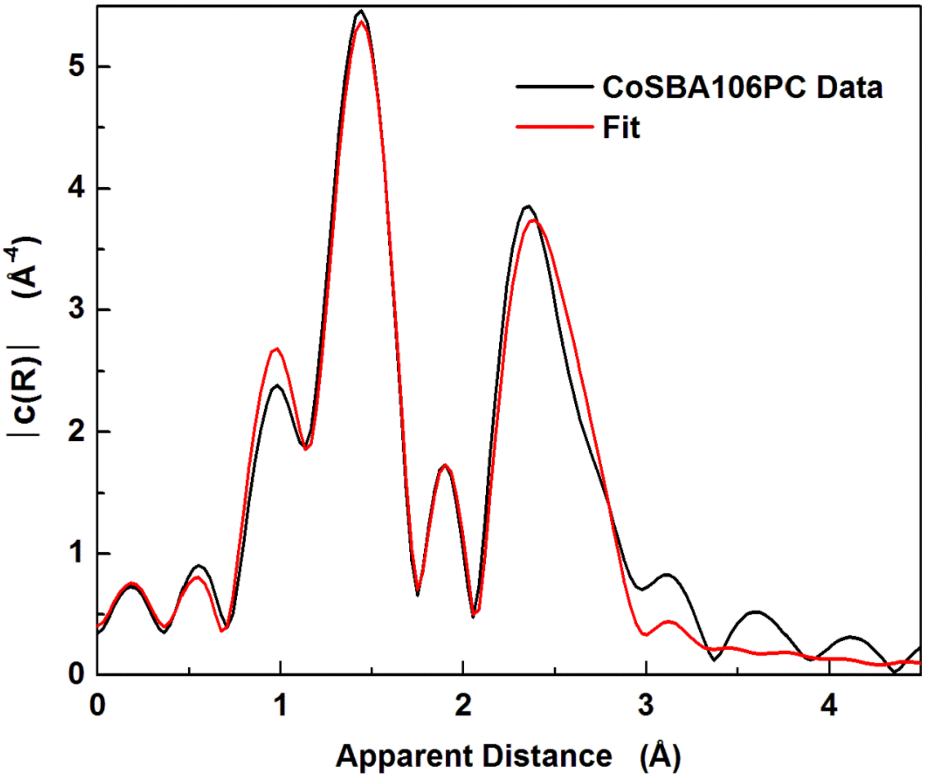

Figure S14. EXAFS fit of CoSBA106 after catalysis is displayed. The EXAFS R-factor (R_f) for the fit is 0.0070 and the reduced χ_v^2 is 28.0. Co-O distance in this model is 1.96 Å with a coordination number (CN) of 5.6. Co-Si distance in this model is 2.77 Å with a CN of 2. Co-Co distance in this model is 2.66 Å with a CN of 1.6.

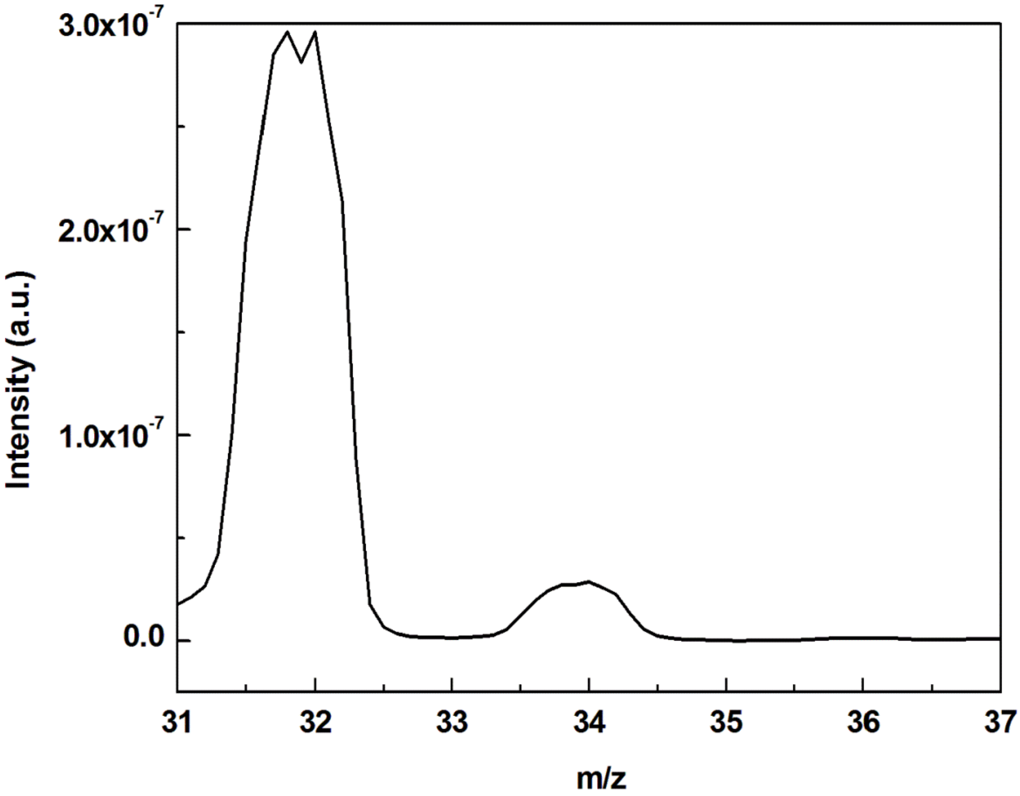

Figure S15. Mass spectrograph of evolved oxygen in an experiment with $H_2{}^{18}O$ (5.5 vol %) employing CoSBA048 as the catalyst. The observed ratio of $^{32}O_2$ and $^{34}O_2$ from the MS data is 8.77, well corresponding to a predicted value from a 5.5 vol % $H_2{}^{18}O$ solution of 8.59. The agreement between the calculated and the observed ratios of $^{32}O_2$ and $^{34}O_2$ indicates that the sole source of O_2 was water.

Table S1. Isotopic product distribution and calculated yields of an ^{18}O labeling experiment.

	$H_2{}^{18}O/H_2{}^{16}O$ v/v %	$^{16}O_2$	$^{16}O^{18}O$	$^{18}O_2$
Measured	5.5 ± 0.9	89.8 ± 7.9	10.2 ± 2.1	trace*
Calculated		89.3	10.4	0.3

*****Note: $^{18}O_2$ detected had poor S/N such that the integration of the peak was not reliable.

Table S2. EXAFS curve fitting results of CoSBA samples.

Fit	**Path**	**R (Å)**	**N**	**σ^2 (Å^{-2})**	**ΔE_0 (eV)**	**Reduced χ_v^2**	**R_f (%)**
CoSBA027	Co-O	2.07 (0.014)	5.0	0.009 (0.002)	5.2 (1.1)	32.9	1.6
	Co-Si	3.26 (0.033)	2.0	0.005 (0.004)			
	Co-Co	2.82 (0.030)	0.4	0.007 (0.003)			
CoSBA048	Co-O	2.04 (0.011)	5.0	0.010 (0.001)	2.0 (1.0)	42.8	5.3
	Co-Si	3.27 (0.024)	2.0	0.007 (0.003)			
	Co-Co	2.93 (0.044)	0.5	0.006 (0.004)			
CoSBA106	Co-O	2.09 (0.009)	5.0	0.010 (0.001)	0.3 (0.7)	9.3	4.3
	Co-Si	3.29 (0.017)	2.0	0.016 (0.007)			
	Co-Co	2.89 (0.007)	1.2	0.003 (0.001)			
CoSBA332	Co-O	2.02 (0.012)	5.0	0.010 (0.002)	3.6 (1.1)	65.7	6.8
	Co-Si	3.12 (0.036)	2.0	0.016 (0.004)			
	Co-Co	3.04 (0.031)	2.3	0.004 (0.003)			
CoSBA106PC	Co-O	1.96 (0.020)	5.6	0.011 (0.003)	3.2 (2.0)	28.0	7.0
	Co-Si	2.77 (0.056)	2.0	0.004 (0.002)			
	Co-Co	2.66 (0.016)	1.6	0.015 (0.010)			

Fitting region : $1 \leq R$ (Å) ≤ 5.5, $2.5 \leq k$ (Å^{-1}) ≤ 11.5

References

(1) Fujdala, K. L.; Tilley, T. D. *J. Am. Chem. Soc.* **2001**, 123, 10133.
(2) Newville, M.; Boyanov, B. I.; Sayers, D. E. *J. Synchrotron Rad*. **1999**, 6, 264.
(3) Newville, M. *J. Synchrotron Rad*. **2001**, 8, 322.
(4) Ravel, B.; Newville, M. *J. Synchrotron Rad*. **2005**, 12, 537.